Article details

Absolute upconversion quantum yields of blue-emitting LiYF$_4$:Yb^{3+},Tm^{3+} upconverting nanoparticles†

Michael S. Meijer, [ID] [a] Paola A. Rojas-Gutierrez, [ID] [b] Dmitry Busko, [c] Ian A. Howard, [ID] [cd] Florian Frenzel, [e] Christian Würth, [ID] [e] Ute Resch-Genger, [ID] [e] Bryce S. Richards, [ID] [cd] Andrey Turshatov, [ID] [c] John A. Capobianco [ID] *[b] and Sylvestre Bonnet [ID] *[a]

The upconversion quantum yield (Φ_{UC}) is an essential parameter for the characterization of the optical performance of lanthanoid-doped upconverting nanoparticles (UCNPs). Despite its nonlinear dependence on excitation power density (P_{exc}), it is typically reported only as a single number. Here, we present the first measurement of absolute upconversion quantum yields of the individual emission bands of blue light-emitting LiYF$_4$:Yb^{3+},Tm^{3+} UCNPs in toluene. Reporting the quantum yields for the individual emission bands is required for assessing the usability of UCNPs in various applications that require upconverted light of different wavelengths, such as bioimaging, photocatalysis and phototherapy. Here, the reliability of the Φ_{UC} measurements is demonstrated by studying the same batch of UCNPs in three different research groups. The results show that whereas the total upconversion quantum yield of these UCNPs is quite high—typically 0.02 at a power density of 5 W cm^{-2}—most of the upconverted photon flux is emitted in the 794 nm upconversion band, while the blue emission band at 480 nm is very weak, with a much lower quantum yield of $\sim 6 \times 10^{-5}$ at 5 W cm^{-2}. Overall, although the total upconversion quantum yield of LiYF$_4$:Yb^{3+},Tm^{3+} UCNPs seems satisfying, notably for NIR bioimaging, blue-light demanding phototherapy applications will require better-performing UCNPs with higher blue light upconversion quantum yields.

Introduction

Lanthanoid-doped upconverting nanoparticles (UCNPs) have attracted much attention over the last two decades as a result of their wide range of potential applications in bio-imaging and biosensing,[1–4] drug delivery,[5] phototherapy,[6–9] optical thermometry,[10–12] photocatalysis,[13–15] photovoltaics,[16] or security.[17] These nanomaterials show multiple sharp emission bands in the visible region of the spectrum upon sequential absorption of two or more near-infrared (NIR) photons, a non-linear process known as photon upconversion (UC). Typically, UCNPs have a crystalline fluoride host lattice, such as NaYF$_4$, doped with one or more lanthanoid ions. Most commonly, Yb^{3+} ions, capable of absorbing NIR light around 980 nm, are used as sensitizers, while secondary dopants, *e.g.* Er^{3+}, Tm^{3+}, or Ho^{3+} ions, are introduced in the crystal lattice as emitting activators, depending on the desired emission wavelength(s).[18–20] Compared to other upconverting systems, such as triplet–triplet annihilation upconversion (TTA-UC), UCNPs show long (ms) luminescence lifetimes, high photostability, insensitivity towards molecular oxygen, and no photoblinking.[21,22] In bio-imaging and phototherapy the use of NIR excitation is highly beneficial as it eliminates background fluorescence and reduces scattering, with the advantage of increased penetration depth of the excitation light.[23]

Initially, the main drawbacks of UCNPs were their low absorption cross-section and low internal upconversion photoluminescence quantum yields (Φ_{UC}); high excitation power densities ($P_{exc} > 20$ W cm^{-2}) were often required to effectively trigger photochemical reactions using UCNPs.[24] In response to this shortcoming, a multitude of innovative strategies have

^{a} *Leiden Institute of Chemistry, Leiden University, Gorlaeus Laboratories, P.O. Box 9502, 2300 RA Leiden, The Netherlands. E-mail: bonnet@chem.leidenuniv.nl*

^{b} *Department of Chemistry and Biochemistry, and Centre for NanoScience Research, Concordia University, Montreal, Quebec, H4B 1R6, Canada. E-mail: john.capobianco@concordia.ca*

^{c} *Institute of Microstructure Technology, Karlsruhe Institute of Technology, Hermann-von-Helmholtz-Platz 1, 76344 Eggenstein-Leopoldshafen, Germany*

^{d} *Light Technology Institute, Karlsruhe Institute of Technology, Engesserstrasse 13, 76131 Karlsruhe, Germany*

^{e} *Federal Institute for Materials Research and Testing (BAM), Division Biophotonics, Richard-Willstätter-Straße 11, 12489 Berlin, Germany*

† Electronic supplementary information (ESI) available. See DOI: 10.1039/c8cp03935f

22556 | *Phys. Chem. Chem. Phys.*, 2018, **20**, 22556–22562

This journal is © the Owner Societies 2018

been developed to increase the brightness of UCNPs, such as the application of core–shell structures or decoration of the surface with dyes to increase light absorption.[25–28] As a result of these efforts, 10- to 500-fold enhancement of the luminescence intensity has been reported, which appears to bring UCNPs to the efficiency level of other UC systems, such as those based on triplet–triplet annihilation upconversion (TTA-UC) that typically require P_{exc} on the level of mW cm^{-2}.[29–31] Yet still, the daily practice requires several W cm^{-2} of NIR light to obtain significant effects in phototherapy using UCNPs, in particular when large amounts of blue or UV light are required. The aim of this collaborative paper was to investigate where this apparent discrepancy comes from; for example, why do systems containing UCNPs that show $\sim$2% overall Φ_{UC} still require long irradiation times ($>$2 h) and high P_{exc} to trigger blue-light sensitive photoreactions?

For a long time, most studies have focused on reporting upconversion intensities relative to other batches of UCNPs prepared in the same research laboratory. The broad range (from the UV to the NIR) and anti-Stokes nature of UCNP emission render the determination of quantum yields relative to a reference, such as an organic dye, very difficult,[32] thereby eliminating the method commonly used for the determination of the quantum yields of molecular dye solutions or dispersions of semiconductor quantum dots.[33] Furthermore, the lack of upconverting reference materials makes it *a priori* difficult to compare upconverting quantum yield values reported by different laboratories. Recently, the number of studies involving absolute measurements of Φ_{UC} has increased, in particular for Er- or Ho-doped UCNPs. This provided not only a few benchmark values, but also shone light upon the effect of excitation power density, particle size, and shell coating on the upconversion quantum yield.[34–43] To the best of our knowledge, the highest upconversion quantum yields for UCNPs were reported for 40 nm LiLuF$_4$:Yb^{3+},Er^{3+} UCNPs (Φ_{UC} = 0.050) and LiLuF$_4$:Yb^{3+},Tm^{3+} UCNPs (Φ_{UC} = 0.072).[44] However, even when absolutely measured Φ_{UC} values are provided, the methodologies for determining them are not always identical, and Φ_{UC} values are not seldom given as a single number without specific mention of the power density used for the measurement – probably for the sake of simplicity.

While some studies exist that report on the relative efficiencies of thulium(III) emission lines,[10,45,46] these studies rarely provide absolutely measured Φ_{UC} values for these individual emission lines. Furthermore, as the NIR emissions in Tm-doped materials are known to be multiple orders of magnitude more intense than the blue emissions,[20,47,48] the efficiency of the blue emission bands cannot easily be deduced from their overall Φ_{UC},[49] and thus remains essentially unknown.

This situation, and the lively discussions within the European COST Action 1403 on upconverting materials, encouraged us to assess the Φ_{UC} of the individual upconversion bands of LiYF$_4$:Yb^{3+},Tm^{3+} UCNPs. LiYF$_4$ was selected as it has been proposed as a very efficient host lattice for Tm-based UC nanomaterials, but its efficiency had not yet been studied with absolute methods.[50] In order to also assess the challenges and factors governing the reliability of such measurements, we independently determined

the Φ_{UC} of the UCNPs in three European research groups (in Leiden, Karlsruhe, and Berlin) using absolute integrating sphere setups of different complexity. We discuss herein the setups, methodologies, and data from the three groups, to identify which parameters must be controlled for providing accurate and reliable Φ_{UC} values. The effects of power density, temperature, and excitation wavelength on the Φ_{UC} values are also discussed.
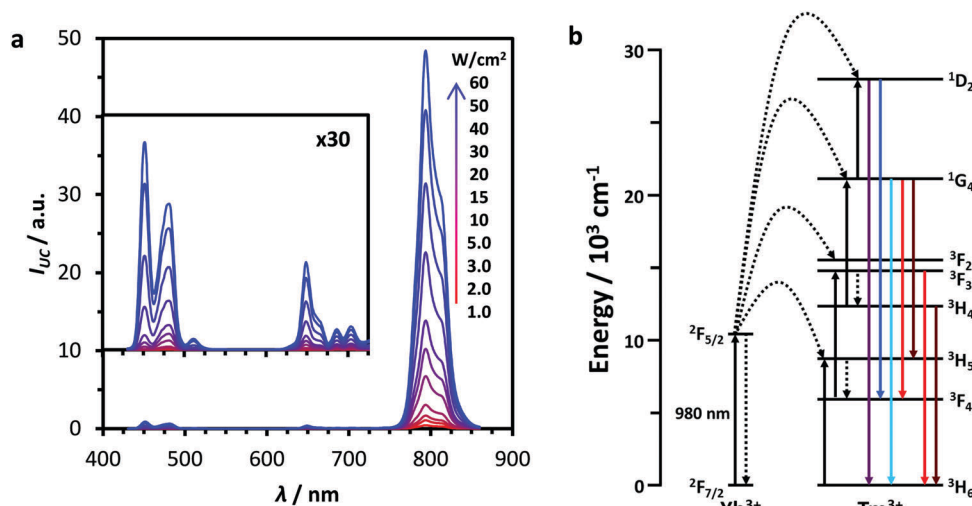
Results and discussion

The tetragonal LiYF$_4$:Yb^{3+},Tm^{3+} (25% Yb^{3+}, 0.5% Tm^{3+}) UCNPs were synthesized as reported following a two-step thermal decomposition procedure.[50,51] Using transmission electron microscopy (TEM) it was shown that these oleate-capped UCNPs have a diamond-like morphology with an average size of 87 $\pm$ 9 nm along the long diagonal and 50 $\pm$ 4 nm along the short diagonal. A second batch of LiYF$_4$ nanoparticles was synthesized without the lanthanoid dopants. These undoped nanoparticles showed a morphology and size (87 $\pm$ 6 nm by 48 $\pm$ 3.5 nm) similar to the doped UCNPs, and served as a blank sample for some of the Φ_{UC} determinations (*vide infra*). Powder X-ray diffraction (XRD) spectra, TEM images and size distributions are shown in the ESI† (Fig. S1–S3). Under NIR light excitation the UC emission spectrum of the Tm-doped UCNPs is clearly dominated by an emission band around 794 nm (Fig. 1). This emission stems mainly from the thulium $^3H_4 \rightarrow {}^3H_6$ transition, with a small contribution from the $^1G_4 \rightarrow {}^3H_5$ transition. In addition, several blue and red Tm-based emission features are present, most notably around 451 nm ($^1D_2 \rightarrow {}^3F_4$), 480 nm ($^1G_4 \rightarrow {}^3H_6$), and 649 nm ($^1G_4 \rightarrow {}^3F_4$). These emission bands are caused by three- and four-photon upconversion processes, and are multiple orders of magnitude less intense than the 794 nm emission band, resulting predominantly from a two-photon process.

The efficiency of the upconversion process in LiYF$_4$:Yb^{3+}, Tm^{3+} UCNPs in toluene dispersion was assessed by measuring Φ_{UC} absolutely, as defined by eqn (1).

$$\Phi_{UC} = \frac{\text{number of photons emitted}}{\text{number of photons absorbed}} = \frac{q_{\text{p-em}}}{q_{\text{p-abs}}} \quad (1)$$

In this equation, $q_{\text{p-em}}$ is the upconverted emission photon flux (in photons s^{-1}) and $q_{\text{p-abs}}$ is the photon flux absorbed by the sensitizer species (in photons s^{-1}). The assessment of Φ_{UC} was performed independently by the Leiden, Karlsruhe and Berlin research groups, using their respective standard methods and instrumentation. All three groups employed measurement setups comprising of integrating spheres and fiber-coupled CCD spectrometers. Continuous wave (CW) laser diodes were used as the excitation source in all setups, although varying slightly in excitation wavelength. In Leiden, a 969 nm laser diode was employed, whereas excitation in Karlsruhe and Berlin was performed at 980 and 976 nm, respectively.

Measurements in Leiden were performed using the method described by Boyer and Van Veggel.[34] An sample of LiYF$_4$ UCNPs of similar size and morphology but without dopant was utilized

This journal is © the Owner Societies 2018

Phys. Chem. Chem. Phys., 2018, **20**, 22556–22562 | 22557

Fig. 1 (a) Emission intensity (I_{UC}) of LiYF$_4$:Yb^{3+},Tm^{3+} (25%, 0.5%) UCNPs in toluene (10 mg mL^{-1}) recorded in Leiden at various P_{exc} (1.0–60 W cm^{-2}, λ_{exc} = 969 nm, T = 293 K). Comparable results were obtained in Karlsruhe and Berlin (Fig. S6, ESI†). (b) Simplified energy level diagram depicting the energy transfer upconversion mechanism in Yb,Tm-based UCNPs, and the observed 4f–4f transitions.

as blank to ensure correction for the scattering properties of the UCNPs. In Karlsruhe, the three-measurement (3M) method previously described by De Mello et al. was used.[52,53] Rather than measuring a blank sample, in this method correction for scattering and the absorption of scattered photons is achieved by performing a series of three measurements, namely (a) irradiation of the empty sphere, (b) irradiation of the sample inside the sphere, but not directly in the path of the excitation beam (indirect excitation), and (c) irradiation of the sample inside the sphere and directly in the beam path (direct excitation). The measurement method utilized in Berlin is similar to the method employed in Leiden, and has been described previously.[36] In all systems, absorption and emission measurements were conducted separately in order to cope with the significant difference in intensity between the excitation light and the UC emission. Φ_{UC} values were measured at a high UCNP concentration (up to 40 mg mL^{-1}) to ensure sufficient absorption (3–6%) of the excitation light. A full description of all three measurement setups is

given in the ESI† (Sections S3–S7), and the resulting Φ_{UC} values are reported in Table 1 and Table S1 (ESI†).

The total internal upconversion photoluminescence quantum yield ($\Phi_{UC,total}$), determined by the integration of the UC spectra from 430 to 860 nm, at an excitation power density of 5.0 W cm^{-2} was determined to be 0.026 ± 0.008 in Leiden, which is in good agreement with the value found in Karlsruhe (0.025 ± 0.003), and slightly above the value found in Berlin (0.0189 ± 0.0005, P_{exc} = 5.5 W cm^{-2}). As explained above, it would be tempting to use $\Phi_{UC,total}$ as the sole way to quantify the efficiency of the UCNPs. However, in most applications only a fraction of the emission spectrum can be used. For example, if a dye or light-activated compound only absorbs blue light, then the 794 nm emission is not useful. Therefore, it can be much more relevant to report the Φ_{UC} values for the individual emission bands, as shown in Table 1 and Table S1 (ESI†). For example, at a P_{exc} of 5 W cm^{-2}, the blue emission bands around 451 and 480 nm account only for 0.02–0.06% and 0.2–0.3% of the total UC emission, respectively,

Table 1 Upconversion photoluminescence quantum yields (Φ_{UC}) for LiYF$_4$:Yb^{3+},Tm^{3+} UCNPs. Leiden data points for P_{exc} = 0.07, 1.0 and 50 W cm^{-2} were measured relative to the absolute value at 5.0 W cm^{-2}; T = 293 K. The full data sets are shown in Table S1 (ESI)

	P_{exc} [W cm^{-2}]	$\Phi_{UC,451}$	$\Phi_{UC,480}$	$\Phi_{UC,649}$	$\Phi_{UC,794}$	$\Phi_{UC,total}$
Leiden[a]	0.07	n.d.	n.d.	n.d.	0.009(3)	0.009(3)
	1.0	6(2) × 10^{-7}	2.1(7) × 10^{-5}	1.1(4) × 10^{-5}	0.019(6)	0.019(6)
	5.0	7(2) × 10^{-6}	7(2) × 10^{-5}	3.3(10) × 10^{-5}	0.026(8)	0.026(8)
	50	2.3(7) × 10^{-4}	2.8(9) × 10^{-4}	1.4(5) × 10^{-4}	0.035(11)	0.035(11)
Karlsruhe[b]	0.20	n.d.	n.d.	n.d.	0.009(1)	0.009(1)
	0.95	n.d.	n.d.	n.d.	0.017(2)	0.017(2)
	5.0	1.6(10) × 10^{-5}	6.3(18) × 10^{-5}	n.d.	0.025(3)	0.025(3)
	13.5	4.5(14) × 10^{-5}	1.2(2) × 10^{-4}	6.7(19) × 10^{-5}	0.029(3)	0.029(3)
Berlin[c]	5.5	3.0 × 10^{-6}	4.48(2) × 10^{-5}	2.54(3) × 10^{-5}	0.0188	0.0189(5)
	48	9.08(5) × 10^{-5}	1.65(1) × 10^{-4}	8.48(5) × 10^{-5}	0.0255	0.0260(6)
	212	7.1 × 10^{-4}	5.15(3) × 10^{-4}	2.63 × 10^{-4}	0.0310	0.034(2)
	395	1.37 × 10^{-3}	8.78(2) × 10^{-4}	4.24(1) × 10^{-4}	0.0325	0.0371(7)

[a] λ_{exc} = 969 nm. [b] λ_{exc} = 980 nm. [c] λ_{exc} = 976 nm; n.d.: not determined. Uncertainties on the final digit are presented in parantheses.

while 99.4% of the UC emission stems from the 2-photon NIR emission band around 794 nm. As a NIR-to-blue upconverting system at this P_{exc}, these UCNPs are thus best characterized by their blue emission quantum yield ($\Phi_{UC,blue}$) of 4.8–7.9 × 10^{-5}, rather than by their more encouraging total emission quantum yield ($\Phi_{UC,total}$) of 0.019–0.026.

Another difficulty in reporting and comparing upconversion quantum yields is that Φ_{UC} is highly dependent on the power density of the excitation beam, as upconversion is a non-linear multiphoton process. At low P_{exc}, the observed emission intensity, I_{UC}, is proportional to P^n, where P is the excitation power density, and n is the so-called slope factor, indicative of the number of photons involved in the process.[54,55] Hence, on a log–log plot, I_{UC} is proportional to n, where n is the slope of the linear least-squares curve through the data points (Fig. S4 and S7, ESI†). As P_{exc} increases, saturation of the intermediate excited states occurs, and n slowly reduces to 1. As the upconversion quantum yield, Φ_{UC}, is proportional to $P^{(n-1)}$, it becomes constant at high P_{exc}; a regime often referred to as the saturation regime. Ideally, Φ_{UC} is measured in this saturated regime, where the value is maximal, and less dependent on P_{exc}. However, as Yb,Tm-doped UCNPs show multiple emission bands, each with their own power dependency, it is impossible to determine a single saturation point for the whole system. Furthermore, complete saturation of all these emission bands will not be observed unless extremely high P_{exc} are used (>400 W cm^{-2}). Such irradiation conditions are not available with all experimental setups, and generally speaking irrelevant for the intended applications of UCNPs, so that Φ_{UC} reported in many articles, including ours, is typically P_{exc}-dependent.

The P_{exc} dependency of the upconverted emission of the LiYF$_4$:Yb^{3+},Tm^{3+} UCNPs (Fig. 2 and Table 1) was examined for the four dominant emission bands. Using the three different spectroscopic setups, we were able to examine the P_{exc} dependence over three to four orders of magnitude, a larger range than typically possible for most setups. In Karlsruhe and Berlin, Φ_{UC} values were obtained absolutely, following the same protocol described above. In Leiden, limitations in the output power stability of the laser diode precluded direct Φ_{UC} measurements at high P_{exc}. Thus, the emission intensity was measured relative to the emission intensity at 5.0 W cm^{-2}, and subsequently converted to a Φ_{UC} value using the absolute Φ_{UC} values determined at 5.0 W cm^{-2}. Importantly, despite the differences in setup design and measurement protocols, the results from the different groups are in very good agreement.

In spite of this good overall agreement, we did observe that the Φ_{UC} values obtained on the Berlin setup are typically somewhat lower than those obtained in Leiden and Karlsruhe (Fig. 2). We believe that this may, in part, be attributed to the difference in beam profile used for the measurements. Whereas the measurements in Berlin were performed using a top-hat beam profile, the other setups employed more commonly used near-Gaussian beam profiles. As a result of the Gaussian beam profile, the P_{exc} is not homogeneous throughout the sample, and thus, at many points in the sample, deviates from the reported average P_{exc}. Due to the multiphotonic nature of the upconversion process, these deviations lead to local variations in upconversion efficiency throughout the sample that have been shown to potentially result in a higher apparent (i.e. spatially averaged) Φ_{UC}, especially in the unsaturated P_{exc}-regime.[36]

For the two-photon $^3H_4 \rightarrow ^3H_6$ emission band at 794 nm, the onset of the saturation regime was observed around 0.1 W cm^{-2}, whereafter the slope factor n dropped from 2.5 to about 1.1 (Fig. 2d and Fig. S4, S7e, ESI†). Contributions from the three-photon $^1G_4 \rightarrow ^3H_5$ process to the 794 nm emission band may explain the fact that $n > 2.0$ for low P_{exc}, as well as the incomplete

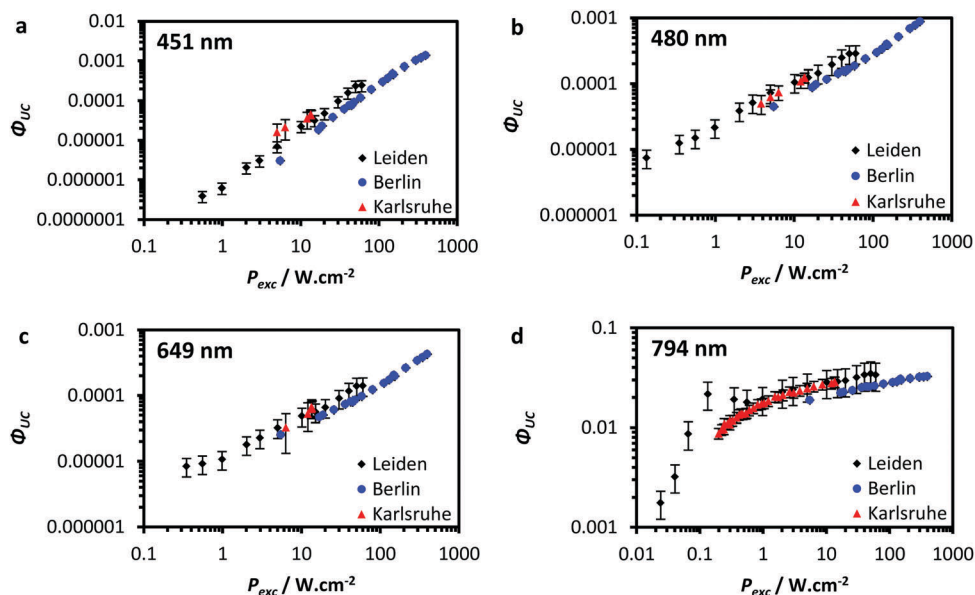**Fig. 2** P_{exc} dependence of Φ_{UC} of the thulium emission bands at (a) 451 nm, (b) 480 nm, (c) 649 nm, and (d) 794 nm in LiYF$_4$:Yb^{3+},Tm^{3+} UCNPs in toluene, measured in Leiden (black diamonds), Berlin (blue circles), and Karlsruhe (red triangles).

This journal is © the Owner Societies 2018

Phys. Chem. Chem. Phys., 2018, **20**, 22556–22562 | 22559

saturation ($n > 1.0$) at higher P_{exc}.[46] No saturation is found for the three major visible bands, and the slopes in Fig. 2a–c are virtually constant. Close examination of the four-photon blue emission band at 451 nm ($^1D_2 \rightarrow {}^3F_4$) reveals that the slope is reduced from $n = 2.8$ to 2.0 as P_{exc} is increased to 395 W cm^{-2} (Fig. S7e, ESI†). This suggests that the first excited thulium state is saturated, but also indicates that the higher excited states in the thulium ions involved are far from saturation. Similarly, the three-photon emission features around 480 nm ($^1G_4 \rightarrow {}^3H_6$) and 649 nm ($^1G_4 \rightarrow {}^3F_4$), both show a slope factor of 1.6, that changes relatively little over the studied P_{exc} range. As P_{exc} in this study was limited to 395 W cm^{-2}, no saturation values for $\Phi_{UC,451}$, $\Phi_{UC,480}$, and $\Phi_{UC,649}$ can be given. Instead, in Table 1 and Fig. 2, Φ_{UC} for these emission bands are given for various values of P_{exc}. Additionally, the lifetime of the downconverted Yb^{3+} emission at 998 nm ($^2F_{5/2} \rightarrow {}^2F_{7/2}$) was measured in Karlsruhe (Fig. S12, ESI†), and, as expected, was found to decrease upon an increase of P_{exc}, from 0.69 ms ($P_{exc} = 10$ W cm^{-2}) to 0.38 ms ($P_{exc} = 220$ W cm^{-2}).

Although the relative contributions of the visible emission bands increase for higher P_{exc}, at 395 W cm^{-2} the 794 nm emission still makes up 88% of the total emission, with the blue emission bands accounting for 2.4% (480 nm) and 3.7% (451 nm) of the total emission, respectively. The maximal Φ_{UC} measured for the total emission is 0.0371(7) (Berlin, $P_{exc} =$ 394.9(6) W cm^{-2}), while all the individual visible light emission showed quantum yields between 1×10^{-4} and 1.4×10^{-3} (Fig. 2 and Fig. S7, Table 1 and Table S1, ESI†). In comparison, Mousavi et al. recently reported a $\Phi_{UC,794}$ of 0.0039 at 14 W cm^{-2} for NaYF$_4$:Yb^{3+},Tm^{3+} (25%, 0.3%) UCNPs, which makes it tempting to conclude that the LiYF$_4$ host lattice used in this work ($\Phi_{UC,794} = 0.022$–0.029 at 15 $\pm$ 2 W cm^{-2}) is more efficient, at least for NIR-to-NIR upconversion.[32] However, the use of a different solvent (cyclohexane versus toluene), different dopant concentrations, and the smaller size of the NaYF$_4$ particles ($\phi = 32$ nm) preclude a direct comparison between the two values.

When high power densities are used for obtaining blue light, the temperature of the upconverting sample may rise. Thus, the effect of temperature on the relative UC efficiency was examined, performing emission spectroscopy in a temperature-controlled cuvette holder. Although an optimum of the $\Phi_{UC,total}$ was found around 18 °C ($\Phi_{UC,total} = 0.026$), and upon heating the sample to 60 °C a 10% reduction in the overall emission was observed, no strong dependence of $\Phi_{UC,total}$ on the temperature was found (Fig. S11 and Table S2, ESI†). Thus, the temperature is of minor importance for upconversion quantum yields of LiYF$_4$:Yb^{3+},Tm^{3+} UCNPs, compared to the influence of other factors such as the surface coating or the nature of the solvent.[38,51]

Finally, as the Φ_{UC} studies in Leiden and Karlsruhe were performed using different excitation wavelengths (969 and 980 nm, respectively (see Table 1)), also the influence of this parameter on the emission intensity and Φ_{UC} was assessed. Fig. 3a depicts the integrated emission intensity of the NIR and blue emission bands as a function of excitation wavelength (excitation spectrum), which is in good agreement with the absorption spectrum of the LiYF$_4$:Yb^{3+},Tm^{3+} UCNPs (Fig. S10, ESI†). Only small differences in emission intensity can be observed between exciting at 969 and 980 nm. However, the sharp peak in the excitation spectrum in Fig. 3a around 960 nm implies that the UC emission is far brighter at this excitation wavelength, compared to the conventional 980 nm excitation. An explanation of these results can be found by looking at the fine structure of the $^2F_{7/2} \rightarrow {}^2F_{5/2}$ transition in Yb^{3+} ions. Under the influence of the crystal field, the Yb^{3+} energy levels split into a number of so-called Stark splitting levels (four and three levels for $^2F_{7/2}$ and $^2F_{5/2}$, respectively), resulting in several absorption bands corresponding to the $^2F_{7/2}(n = 0) \rightarrow {}^2F_{5/2}(n = 0', 1', 2')$ electronic transitions. The absorption between 970 nm and 990 nm is attributed to the $0 \rightarrow 0'$ transition, whereas the absorption bands near 960 nm and 930 nm correspond to the $0 \rightarrow 1'$ and $0 \rightarrow 2'$ transitions, respectively.[56] The relative intensity of these transitions is strongly influenced by the symmetry of
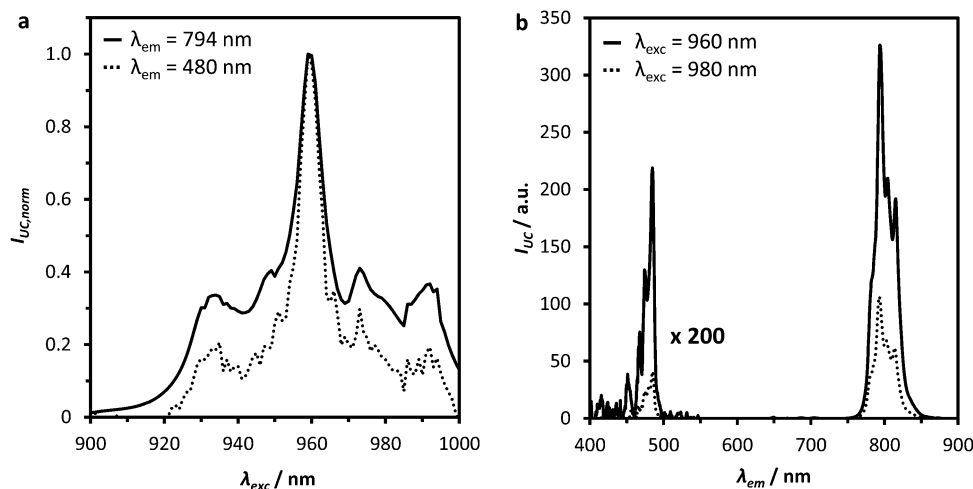

Fig. 3 (a) Normalized excitation spectrum recorded in Karlsruhe of LiYF$_4$:Yb^{3+},Tm^{3+} UCNPs in toluene (10 mg mL^{-1}) for 480 nm and 794 nm emission bands. Spectra were corrected for the small difference in P_{exc}, assuming $n = 1.1$ (794 nm) and 1.6 (480 nm). (b) Upconverted emission spectra recorded in Karlsruhe of LiYF$_4$:Yb^{3+},Tm^{3+} UCNPs in toluene (10 mg mL^{-1}) at various excitation wavelengths ($P_{exc} = 4.11$ W cm^{-2} (960 nm), 4.15 W cm^{-2} (980 nm)).

22560 | Phys. Chem. Chem. Phys., 2018, 20, 22556–22562

This journal is © the Owner Societies 2018

the host lattice. Here, the tetragonal LiYF$_4$ host (scheelite structure) favors the $0 \rightarrow 1'$ transition, in contrast to the hexagonal NaYF$_4$ host, for which the $0 \rightarrow 0'$ transition is dominant. The preference towards the $0 \rightarrow 1'$ transition has been demonstrated before for LiYF$_4$ single crystals doped with Yb^{3+} ions.[56,57] Thus, in order to achieve maximal upconversion brightness, evaluation of the optimal excitation wavelength is crucial for every new host material. In the case of LiYF$_4$, the emission intensities of the NIR and blue UC bands increased considerably upon 960 nm excitation, by a factor of $\sim$3 for the NIR emission and $\sim$6 for the blue emission compared to 980 nm excitation at the used excitation power density (Fig. 3b). Considering the good agreement between the excitation spectrum depicted in Fig. 3a and the absorption spectrum in Fig. S10 (ESI†), we assume that the observed increase in UC emission intensity is caused by the increased absorption at 960 nm, rather than by a significant increase in Φ_{UC}.

Conclusions

In this work, we have presented the first multicenter absolute measurement of upconversion photoluminescence quantum yields (Φ_{UC}) of UCNPs, and provided the first Φ_{UC} values for LiYF$_4$:Yb^{3+},Tm^{3+} UCNPs. These measurements have been performed independently by three research groups, but using the same batch of nanomaterials. In spite of the quite different setups and methods used in the three labs, strikingly similar values were obtained, which underline that these measurements can give reproducible results not only when using state-of-the-art setups such as those available in Karlsruhe and Berlin, but also using relatively inexpensive, modular spectroscopy setups such as the one in Leiden. Importantly, upconversion quantum yield values are given for the individual upconversion bands of LiYF$_4$:Yb^{3+},Tm^{3+} UCNPs. By doing so we illustrate, as done recently for Yb,Er-doped UCNPs,[36,38,41] the strikingly large difference in intensity between the different emission bands of these UCNPs. Although Tm-doped UCNPs are usually described as blue-emitting UCNPs, Φ_{UC} of the blue emission bands are as low as 1×10^{-5} at 5 W cm^{-2}, while the NIR band at 794 nm has an excellent Φ_{UC} of $\sim$0.02 at 5 W cm^{-2}. This discrepancy is especially important when selecting upconverting materials for different applications.[58] In security or bioimaging applications where the 794 nm emission is used, $\Phi_{UC,total}$ is a good measure for the efficiency of LiYF$_4$:Yb^{3+},Tm^{3+} UCNPs, because the upconverted emission spectrum is strongly dominated by the 794 nm band. However, in phototherapeutic applications where only the blue thulium emission is used, for example in the activation of blue-light sensitive anticancer compounds,[59] the actual efficiency of these UCNPs is one to three orders of magnitude lower than $\Phi_{UC,total}$. Thus, reporting only the latter would give a misleading evaluation of the amount of excitation light needed to obtain a measurable photochemical effect *via* NIR-to-blue upconversion. The low efficiency of the blue upconverted emission in Tm-based UCNPs provides a good explanation why these systems are still difficult to apply in for example blue light-triggered phototherapy,[24] and justifies the need for further material research aimed at increasing the upconversion quantum yields of UCNPs in the blue region of the spectrum.

Conflicts of interest

The authors declare no competing financial interest.

Acknowledgements

References

1 R. Wang and F. Zhang, in *Near-infrared Nanomaterials: Preparation, Bioimaging and Therapy Applications*, ed. F. Zhang, The Royal Society of Chemistry, 2016, ch. 1, pp. 1–39.

2 T. Näreoja, T. Deguchi, S. Christ, R. Peltomaa, N. Prabhakar, E. Fazeli, N. Perälä, J. M. Rosenholm, R. Arppe, T. Soukka and M. Schäferling, *Anal. Chem.*, 2017, **89**, 1501–1508.

3 L. Mattsson, K. D. Wegner, N. Hildebrandt and T. Soukka, *RSC Adv.*, 2015, **5**, 13270–13277.

4 C. Drees, A. N. Raj, R. Kurre, K. B. Busch, M. Haase and J. Piehler, *Angew. Chem., Int. Ed.*, 2016, **55**, 11668–11672.

5 A. Bagheri, H. Arandiyan, C. Boyer and M. Lim, *Adv. Sci.*, 2016, **3**, 1500437.

6 K. Deng, C. Li, S. Huang, B. Xing, D. Jin, Q. Zeng, Z. Hou and J. Lin, *Small*, 2017, **13**, 1702299.

7 E. Ruggiero, S. Alonso-deCastro, A. Habtemariam and L. Salassa, *Dalton Trans.*, 2016, **45**, 13012–13020.

8 D. Wang, B. Xue, X. Kong, T. Langping, X. Liu, Y. Zhang, Y. Chang, Y. Luo, H. Zhao and H. Zhang, *Nanoscale*, 2015, **7**, 190–197.

9 Z. Chen, R. Thiramanas, M. Schwendy, C. Xie, S. H. Parekh, V. Mailänder and S. Wu, *Small*, 2017, **13**, 1700997.

10 W. Chen, C. Shi, T. Tao, M. Ji, S. Zheng, X. Sang, X. Liu and J. Qiu, *RSC Adv.*, 2016, **6**, 21540–21545.

This journal is © the Owner Societies 2018

Phys. Chem. Chem. Phys., 2018, **20**, 22556–22562 | 22561

11 J. D. Kilbane, E. M. Chan, C. Monachon, N. J. Borys, E. S. Levy, A. D. Pickel, J. J. Urban, P. J. Schuck and C. Dames, *Nanoscale*, 2016, **8**, 11611–11616.

12 A. Sedlmeier, D. E. Achatz, L. H. Fischer, H. H. Gorris and O. S. Wolfbeis, *Nanoscale*, 2012, **4**, 7090–7096.

13 X. Liu, H.-C. Chen, X. Kong, Y. Zhang, L. Tu, Y. Chang, F. Wu, T. Wang, J. N. H. Reek, A. M. Brouwer and H. Zhang, *Chem. Commun.*, 2015, **51**, 13008–13011.

14 Y. Tang, W. Di, X. Zhai, R. Yang and W. Qin, *ACS Catal.*, 2013, **3**, 405–412.

15 Z. Xu, M. Quintanilla, F. Vetrone, A. O. Govorov, M. Chaker and D. Ma, *Adv. Funct. Mater.*, 2015, **25**, 2950–2960.

16 C. L. M. Hofmann, E. H. Eriksen, S. Fischer, B. S. Richards, P. Balling and J. C. Goldschmidt, *Opt. Express*, 2018, **26**, 7537–7554.

17 W. J. Kim, M. Nyk and P. N. Prasad, *Nanotechnology*, 2009, **20**, 185301.

18 J. C. Boyer, F. Vetrone, L. A. Cuccia and J. A. Capobianco, *J. Am. Chem. Soc.*, 2006, **128**, 7444–7445.

19 W. Gao, H. Zheng, Q. Han, E. He and R. Wang, *CrystEngComm*, 2014, **16**, 6697–6706.

20 F. Wang and X. G. Liu, *J. Am. Chem. Soc.*, 2008, **130**, 5642–5643.

21 A. D. Ostrowski, E. M. Chan, D. J. Gargas, E. M. Katz, G. Han, P. J. Schuck, D. J. Milliron and B. E. Cohen, *ACS Nano*, 2012, **6**, 2686–2692.

22 G. Liu, *Chem. Soc. Rev.*, 2015, **44**, 1635–1652.

23 A. N. Bashkatov, E. A. Genina, V. I. Kochubey and V. V. Tuchin, *J. Phys. D: Appl. Phys.*, 2005, **38**, 2543–2555.

24 E. Ruggiero, A. Habtemariam, L. Yate, J. C. Mareque-Rivas and L. Salassa, *Chem. Commun.*, 2014, **50**, 1715–1718.

25 G. Chen, H. Agren, T. Y. Ohulchanskyy and P. N. Prasad, *Chem. Soc. Rev.*, 2015, **44**, 1680–1713.

26 X. Xie, N. Gao, R. Deng, Q. Sun, Q.-H. Xu and X. Liu, *J. Am. Chem. Soc.*, 2013, **135**, 12608–12611.

27 W. Zou, C. Visser, J. A. Maduro, M. S. Pshenichnikov and J. C. Hummelen, *Nat. Photonics*, 2012, **6**, 560–564.

28 D. J. Garfield, N. J. Borys, S. M. Hamed, N. A. Torquato, C. A. Tajon, B. Tian, B. Shevitski, E. S. Barnard, Y. D. Suh, S. Aloni, J. B. Neaton, E. M. Chan, B. E. Cohen and P. J. Schuck, *Nat. Photonics*, 2018, **12**, 402–407.

29 Q. Dou, L. Jiang, D. Kai, C. Owh and X. J. Loh, *Drug Discovery Today*, 2017, **22**, 1400–1411.

30 S. H. C. Askes, P. Brodie, G. Bruylants and S. Bonnet, *J. Phys. Chem. B*, 2017, **121**, 780–786.

31 V. Gray, K. Moth-Poulsen, B. Albinsson and M. Abrahamsson, *Coord. Chem. Rev.*, 2018, **362**, 54–71.

32 M. Mousavi, B. Thomasson, M. Li, M. Kraft, C. Würth, U. Resch-Genger and S. Andersson-Engels, *Phys. Chem. Chem. Phys.*, 2017, **19**, 22016–22022.

33 C. Würth, M. Grabolle, J. Pauli, M. Spieles and U. Resch-Genger, *Nat. Protoc.*, 2013, **8**, 1535–1550.

34 J. C. Boyer and F. C. J. M. van Veggel, *Nanoscale*, 2010, **2**, 1417–1419.

35 S. Fischer, N. J. J. Johnson, J. Pichaandi, J. C. Goldschmidt and F. C. J. M. van Veggel, *J. Appl. Phys.*, 2015, **118**, 193105.

36 M. Kaiser, C. Würth, M. Kraft, I. Hyppanen, T. Soukka and U. Resch-Genger, *Nanoscale*, 2017, **9**, 10051–10058.

37 S. Balabhadra, M. L. Debasu, C. D. S. Brites, R. A. S. Ferreira and L. D. Carlos, *J. Lumin.*, 2017, **189**, 64–70.

38 C. Würth, M. Kaiser, S. Wilhelm, B. Grauel, T. Hirsch and U. Resch-Genger, *Nanoscale*, 2017, **9**, 4283–4294.

39 A. Pilch, B. Czaban, D. Wawrzyńczyk and A. Bednarkiewicz, *J. Lumin.*, 2018, **198**, 482–487.

40 A. Pilch, D. Wawrzyńczyk, M. Kurnatowska, B. Czaban, M. Samoć, W. Strek and A. Bednarkiewicz, *J. Lumin.*, 2017, **182**, 114–122.

41 C. Würth, S. Fischer, B. Grauel, A. P. Alivisatos and U. Resch-Genger, *J. Am. Chem. Soc.*, 2018, **140**, 4922–4928.

42 C. Homann, L. Krukewitt, F. Frenzel, B. Grauel, C. Würth, U. Resch-Genger and M. Haase, *Angew. Chem., Int. Ed.*, 2018, **57**, 8765–8769.

43 M. Y. Hossan, A. Hor, Q. Luu, S. J. Smith, P. S. May and M. T. Berry, *J. Phys. Chem. C*, 2017, **121**, 16592–16606.

44 P. Huang, W. Zheng, S. Zhou, D. Tu, Z. Chen, H. Zhu, R. Li, E. Ma, M. Huang and X. Chen, *Angew. Chem., Int. Ed.*, 2014, **53**, 1252–1257.

45 K. W. Krämer, D. Biner, G. Frei, H. U. Güdel, M. P. Hehlen and S. R. Lüthi, *Chem. Mater.*, 2004, **16**, 1244–1251.

46 M. Quintanilla, I. X. Cantarelli, M. Pedroni, A. Speghini and F. Vetrone, *J. Mater. Chem. C*, 2015, **3**, 3108–3113.

47 S. Heer, O. Lehmann, M. Haase and H. U. Güdel, *Angew. Chem., Int. Ed.*, 2003, **42**, 3179–3182.

48 X. Liu, J. Zhao, Y. Sun, K. Song, Y. Yu, C. Du, X. Kong and H. Zhang, *Chem. Commun.*, 2009, 6628–6630.

49 S. Fischer, J. K. Swabeck and A. P. Alivisatos, *J. Am. Chem. Soc.*, 2017, **139**, 12325–12332.

50 V. Mahalingam, F. Vetrone, R. Naccache, A. Speghini and J. A. Capobianco, *Adv. Mater.*, 2009, **21**, 4025–4028.

51 P. A. Rojas-Gutierrez, C. DeWolf and J. A. Capobianco, *Part. Part. Syst. Charact.*, 2016, **33**, 865–870.

52 D. O. Faulkner, J. J. McDowell, A. J. Price, D. D. Perovic, N. P. Kherani and G. A. Ozin, *Laser Photonics Rev.*, 2012, **6**, 802–806.

53 J. C. de Mello, H. F. Wittmann and R. H. Friend, *Adv. Mater.*, 1997, **9**, 230–232.

54 J. F. Suyver, A. Aebischer, S. García-Revilla, P. Gerner and H. U. Güdel, *Phys. Rev. B: Condens. Matter Mater. Phys.*, 2005, **71**, 125123.

55 M. Pollnau, D. R. Gamelin, S. R. Lüthi, H. U. Güdel and M. P. Hehlen, *Phys. Rev. B: Condens. Matter Mater. Phys.*, 2000, **61**, 3337–3346.

56 A. Sugiyama, M. Katsurayama, Y. Anzai and T. Tsuboi, *J. Alloys Compd.*, 2006, **408-412**, 780–783.

57 L. D. DeLoach, S. A. Payne, L. L. Chase, L. K. Smith, W. L. Kway and W. F. Krupke, *IEEE J. Quantum Electron.*, 1993, **29**, 1179–1191.

58 G. Jalani, R. Naccache, D. H. Rosenzweig, S. Lerouge, L. Haglund, F. Vetrone and M. Cerruti, *Nanoscale*, 2015, **7**, 11255–11262.

59 Q. Yu, E. M. Rodriguez, R. Naccache, P. Forgione, G. Lamoureux, F. Sanz-Rodriguez, D. Scheglmann and J. A. Capobianco, *Chem. Commun.*, 2014, **50**, 12150–12153.

22562 | *Phys. Chem. Chem. Phys.*, 2018, **20**, 22556–22562

This journal is © the Owner Societies 2018